Non-adiabatic Dynamics Between Valence, Non-valence and Continuum Electronic States in a Hetero Polycyclic Aromatic Hydrocarbon

James N. Bull,[*,†] Cate S. Anstöter,[‡] Mark H. Stockett,[¶] Connor J. Clarke,[§]

Jemma A. Gibbard,[§] Evan J. Bieske,[‖] and Jan R. R. Verlet[§]

[†]*School of Chemistry, Norwich Research Park, University of East Anglia, Norwich NR4 7TJ, United Kingdom*

[‡]*Department of Chemistry, Temple University, 1901 N 13th St, Philadelphia, PA 19122, United States*

[¶]*Department of Physics, Stockholm University, Stockholm, Sweden*

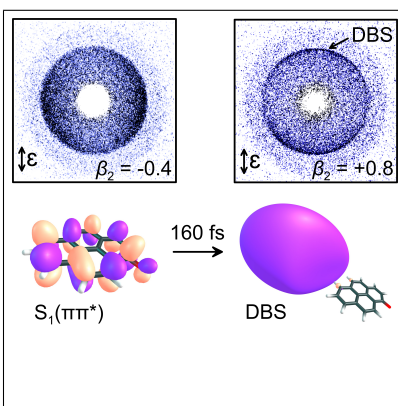[§]*Department of Chemistry, Durham University, Durham, DH1 3LE, United Kingdom*

[‖]*School of Chemistry, University of Melbourne, Melbourne, VIC 3010, Australia*

E-mail: james.bull@uea.ac.uk

Abstract

Internal conversion between valence-localized and dipole-bound states is thought to be a ubiquitous process in polar molecular anions, yet there is limited direct evidence. Here, photodetachment action spectroscopy and time-resolved photoelectron imaging with a hetero polycyclic aromatic hydrocarbon (hetero-PAH) anion, deprotonated 1-pyrenol, is used to demonstrate a sub-picosecond (τ_1=160±20 fs) valence to dipole-bound state internal conversion following excitation of the origin transition of the first valence-localized excited state. The internal conversion dynamics are evident in the photoelectron spectra and in the photoelectron angular distributions (β_2 values) as the electronic character of the excited state population changes from valence to non-valence. The dipole-bound state subsequently decays through mode-specific vibrational autodetachment with lifetime τ_2=11±2 ps. These internal conversion and autodetachment dynamics are likely common in molecular anions, but difficult to fingerprint due to the transient existence of the dipole-bound state. Potential implications of the excited state dynamics for interstellar hetero-PAH anion formation are discussed.

TOC Graphic

The dipole-bound state (DBS), which was first hypothesized in 1947,[1] is a non-valence state of an anion in which an electron is bound beyond a molecule's valence shell by the electric field associated with the dipole moment, μ, of the (neutral) molecular core. The theoretical requirement for whether a molecule can support a DBS is if $|\mu| > 1.625\,\mathrm{D}$, although experiments have suggested that the condition is closer to $|\mu| > 2.0\,\mathrm{D}$ due to molecular rotation and centrifugal effects.[2–4] Despite the DBS lying only 10–100 meV below the detachment threshold,[5,6] it has important roles in interstellar anion formation,[7–9] electron transfer processes in biology,[10,11] and coupling of solute molecules with solvated electrons.[12] Recent studies have suggested that DBSs are important in certain isomerization and dissociation reactions.[13,14] Underpinning each of these examples are the efficient non-adiabatic couplings that funnel population between the valence-localized and dipole-bound state and its interaction with the electronic continuum.

While spectroscopic and electron transfer studies, e.g. collisional resonant electron transfer, often show clear signatures for DBS vibrational progressions,[6,15] the ultrafast dynamics associated with internal conversion between valence-localized and DBSs are largely unstudied. The few exceptions, investigated using femtosecond photoelectron spectroscopy, involve cluster anions with a high degree of conformational fluxionality,[16–19] or excited state processes involving extensive nuclear relaxation.[11] To date, there have been no examples of valence to DBS internal conversion in 'rigid' molecules, i.e. those without fluxionality associated with internal rotations or low-frequency intermoleculer cluster binding modes, or for molecules for which a specific vibronic mode is excited. In an elegant contribution, Kang et al.[20] applied a picosecond time-resolved photoelectron spectroscopy strategy on cryocooled phenoxide to selectively excite DBS vibrations and monitor mode-specific vibrational autodetachment lifetimes (1.4 to 34 ps), however, their time resolution (pump pulse duration $\approx 1.4\,\mathrm{ps}$) is unsuitable for characterizing sub-picosecond internal conversion dynamics.

In the present work, we have used photodetachment action spectroscopy and time-resolved photoelectron imaging at $T \approx 300\,\mathrm{K}$ to investigate the formation and decay dy-

namics of the DBS in a model oxygenated polycyclic aromatic hydrocarbon (PAH), deprotonated 1-pyrenol (Figure 1, Py1$^-$), a molecule which has been recently characterized in the near-threshold electron detachment region using cryogenic photoelectron and photodetachment spectroscopies.[21] Compared with earlier studies on DBS dynamics in clusters and highly fluxional molecules, Py1$^-$ has a rigid carbon backbone and the photodetachment action spectrum for the S$_1$ band is dominated by the origin transition. PAHs and hetero-atom derivatives (hetero-PAHs) are a class of molecules for which DBSs are of particular interest due to their role in interstellar anion formation[7,8] and because of the importance of PAHs as a motif in organic semiconductors.[22] 1-pyrenol is often considered as a prototype astrophysical hetero-PAH on the basis of experiments in which PAH-ice mixtures were subjected to interstellar conditions and VUV irradiation, showing formation of 1-pyrenol, Py1$^-$ and the radical Py1.[23,24] Similar experiments on other PAH-ice mixtures have shown formation of alcohol, ketone and carboxylic acid functional groups,[25–29] suggesting that oxygenated PAHs should contribute to the interstellar organic inventory.

A photodetachment action spectrum for Py1$^-$ is shown in Figure 2a. The spectrum is dominated by a feature centered at 2.602±0.005 eV and is assigned to the 0-0 origin transition (shape resonance)[30] of the S$_1$ band through Franck-Condon-Herzberg-Teller modelling (Figure 2b). The simulations suggest that the origin transition is flanked by hot band vibrations, particularly on the low photon energy shoulder ($h\nu$=2.55–2.60 eV, Supporting Information). The measured 0-0 transition energy agrees with a recent cryogenic photodetachment spec-
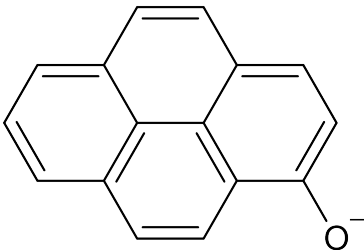

Figure 1: Structure of deprotonated 1-pyrenol (Py1$^-$), a model closed-shell hetero-PAH anion that supports a DBS.

troscopy measurement at 2.6042±0.0006 eV,[21] which found a lifetime broadened line shape with a lower-limit lifetime of ≈50 fs. Three weak spectral features, shown magnified in the inset in Figure 2a, are observed in the near-threshold region: **0** at 2.445±0.005 eV, **4** at 2.495±0.005 eV and **7** at 2.507±0.005 eV, with the labelling convention following Ref. 21. These features are assigned to the ground state DBS and vibrational levels for the DBS which are similar to those for the D_0 electronic state calculated at 422 and 524 cm^{-1} (Supporting Information). The present DBS binding energy at 32±6 meV agrees with the calculated binding energy of 29 meV for the DBS orbital shown in Figure 2c. Weaker spectral features in Figure 2a over the $h\nu$ =2.63–2.80 eV range are consistent with simulated vibronic structure for the S_1 band (Figure 2b) and possibly with the onset of the S_2 band (ca. 2.8–2.9 eV).

The excited state dynamics associated with the origin transition of the S_1 band (TR1 in Figure 2a) were probed using time-resolved photoelectron imaging,[18] involving a $h\nu$=2.60 eV + 1.55 eV pump-probe scheme and with velocity-map images recorded with varying pump-probe delay, Δt. The pump-probe cross correlation was ≈60 fs. Photoelectron spectroscopy using velocity-map imaging detection and image reconstruction algorithms provide the full 3D velocity distribution of the photoelectrons.[31] The photoelectron spectrum and photoelectron angular distributions quantified by the conventional β_2 value are obtained by integrating the central slice of the 3D velocity distribution over the appropriate coordinate and applying a simple velocity-to-energy transformation.[32,33] Parameter β_2 may vary between -1 and +2, corresponding to electron ejection perpendicular and parallel to the laser polarization, ϵ, respectively.

The pump-only photoelectron spectrum and corresponding photoelectron angular anisotropy distribution are shown in Figure 3a. The spectrum has three clear peaks with electron kinetic energy (eKE) centered at 0.03, 0.06 and 0.13 eV; β_2 values are zero over the first two peaks and negative over the third, reaching -0.2 at eKE≈0.13 eV. Such sudden changes in β_2 values imply at least two distinct electron detachment processes,[34,35] with the eKE≈0.13 eV (anisotropic) peak assigned to non-resonant direct photodetachment (DD) based on the
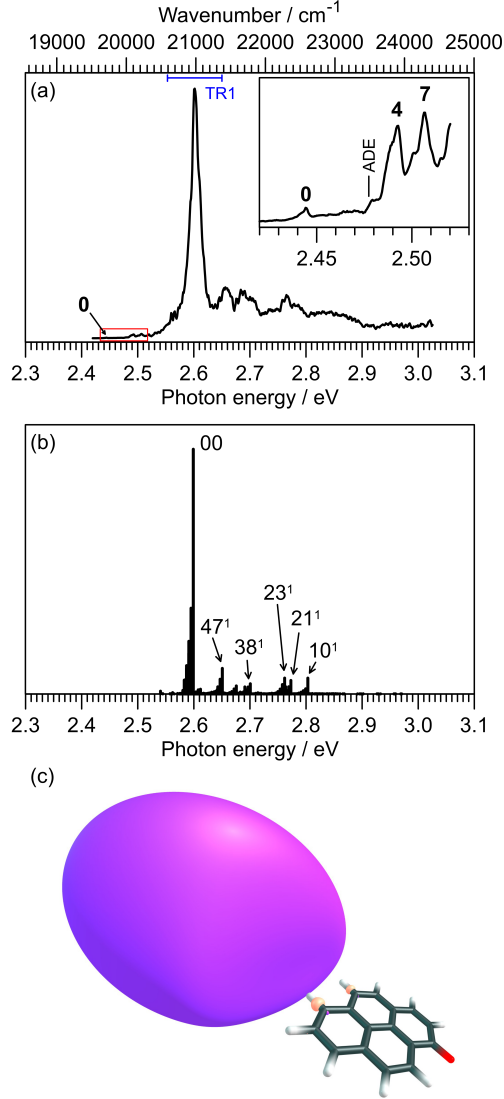
Figure 2: Electronic spectroscopy of Py1$^-$ at $T \approx 300$ K: (a) photodetachment spectrum and near-threshold region (inset). (b) Franck-Condon-Herzberg-Teller modelling of the S$_1$ band, including hot band transitions at $T = 300$ K. (c) illustration of the calculated DBS (0.004 au isosurface); $|\mu|$ for Py1 was calculated as 5.2 D. In (a), ADE is the adiabatic detachment energy at 2.4772±0.0004 eV taken from Ref. 21, and TR1 indicates the femtosecond pump pulse bandwidth (FHWM≈0.1 eV). The photodetachment action spectrum should be a close approximation to the absorption spectrum at $T \approx 300$ K since there was no evidence for photodissociation (Supporting Information), and because time-gated measurements indicate that electron detachment is complete within a few nanoseconds (Supporting Information), i.e. no thermionic emission due to ground state recovery. Complete experimental and theoretical details are given in the Supporting Information.

known ADE[21] and a further set of photoelectron spectra given in the Supporting Informa-

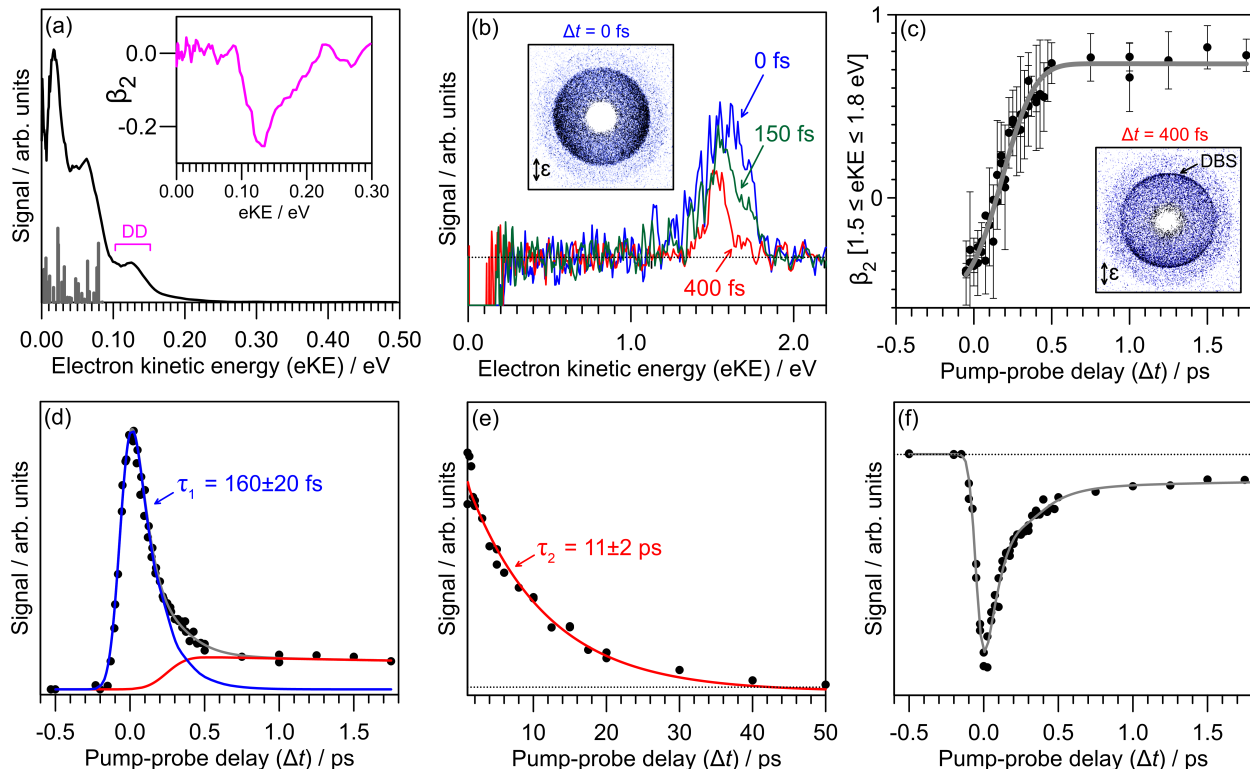tion. In accord with the time-resolved experiments described below, the two lower-eKE peaks
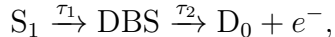
Figure 3: Excited state dynamics following excitation at the origin transition of the S_1 state in Py1$^-$: (a) $h\nu$=2.60 eV (pump only) photoelectron spectrum with photoelectron angular distribution anisotropy (β_2 values) shown in the inset. The vertical bars are a model for VAD (see text). (b) pump-probe spectra at $\Delta t = 0$ fs (blue), 150 fs (green) and 400 fs (red), and with the background-corrected $\Delta t = 0$ fs image shown in the inset. (c) photoelectron angular distribution anisotropy (β_2 values) averaged over the high-eKE feature with Δt, and with the background-corrected $\Delta t = 400$ fs image shown in the inset. Higher order anisotropy parameters, e.g. β_4, are not statistically significant. (d) integrated high-eKE signal for $\Delta t \leq 1.8$ ps and fit with two-component kinetic model ($S_1 \xrightarrow{\tau_1} DBS \xrightarrow{\tau_2} D_0 + e^-$) where blue is population of the S_1 state, red is population of the DBS, and grey is S_1 + DBS population, (e) integrated high-eKE signal over the longer Δt range, (f) low-eKE (photodepeltion) signal for $\Delta t \leq 1.8$ ps fit with the same kinetic model. The weak high velocity ring in the velocity-map images is two-photon pump signal and is constant with Δt. ϵ is the pump laser polarization. Complete experimental details are given in the Supporting Information.

are assigned to mode-specific vibrational autodetachment (VAD), a process that should show isotropic ($\beta_2 = 0$, s-wave) electron ejection.

Time-resolved spectra, which are pump-probe photoelectron spectra corrected for the pump-only background, for $\Delta t = 0.0$, 0.15 and 0.4 ps are shown in Figure 3b. In essence, these time-resolved spectra show evolution of the photoexcited population as a function

of time. There is photodepletion (bleaching) of the low-eKE feature and appearance of signal in the 1.3≤eKE≤1.8 eV range. For the 0≤ Δt ≤100 fs time-resolved spectra, the photoappearance feature is broad with a negative β_2 value (Figure 3c). The negative β_2 value is consistent with detachment from a π orbital and with electron ejection perpendicular to the laser polarization, i.e., perpendicular to the in-plane transition dipole moment for photoexcitation. With increasing Δt, the high-eKE feature sharpens to a peak centered just below the probe photon energy at eKE≈1.5 eV and with concomitant increase of β_2 values toward an asymptotic value at β_2=+0.8±0.1 by Δt ≈500 fs. Evolution of the high-eKE feature from a broad photoelectron spectrum into a sharp, anisotropic spectrum with p-wave detachment character and with a binding energy of a few tens of milli-electron volts is consistent with internal conversion to an s-like DBS.[11,18] It is worth noting that while β_2 = +2 is the limiting value for electron ejection parallel to the femtosecond laser polarization axis associated with a pure p-wave, β_2 values for detachment from a DBS are usually closer to β_2 = +1 due to the angular momentum and $s - p$ orbital mixing reasons detailed in Ref. 35. To the authors' knowledge, the sub-picosecond evolution of β_2 values for Py1$^-$ in this work provide the clearest example to date of ultrafast changes in photoelectron angular distributions obtained using anion time-resolved photoelectron imaging.

Integrated signal for the high-eKE feature out to Δt=1.8 ps is shown in Figure 3d, with the longer Δt range shown in Figure 3e. Taking into account the femtosecond pulse cross-correlation, the integrated signal was fit with a two-component (S$_1$ and DBS) kinetic model assuming first-order decay from the S$_1$ state to the DBS, followed by VAD from the DBS:[36]

$$S_1 \xrightarrow{\tau_1} DBS \xrightarrow{\tau_2} D_0 + e^-,$$

where D$_0$ is the ground electronic state of neutral Py1. The kinetic model does not require that all S$_1$ signal evolves into DBS signal for two reasons: (1) some S$_1$ population may autodetach before internal conversion, (2) the probe photodetachment cross-sections for the S$_1$ state and DBS may differ. Fitted lifetimes from the kinetic model are $\tau_1 = 160 \pm 20$ fs and

$\tau_2 = 11 \pm 2\,\text{ps}$. Integrated time-resolved photodepletion signal is shown in Figure 3f, which fits well to the same kinetic model and confirms that the DBS decay in the single-photon (pump only) spectrum is associated decay of the DBS.

The mechanism for decay of the DBS over the picosecond timescale is mode-specific VAD. The theory for mode-specific VAD is well established,[35,37,38] and has been characterized for DBS decay in cryogenic,[14,15,21,39,40] $T \approx 300\,\text{K}$,[11,18] and highly-excited anions.[41] Briefly, the mechanism involves vibrational motion causing modulation of the dipole-bound state orbital (i.e., direction and magnitude of the dipole moment) and resulting in an electron 'shake-off' with the outgoing electron kinetic energy proportional to the mode frequency and selection rule $\Delta \nu = -1$, where ν is the vibrational quantum number. Since Py1$^-$ was excited at the origin transition of the S$_1$ band, the vibrational energy may come from two sources: (1) electronic-to-vibrational energy conversion associated with internal conversion to the DBS ($\approx 0.16\,\text{eV}$ from Figure 2a), and (2) the initial average thermal energy of the anions calculated as $\approx 0.22\,\text{eV}$ from a harmonic oscillator partition function at $T = 300\,\text{K}$. Because source (2) is expected to dominate on ultrafast timescales, the VAD spectrum was modelled assuming vibrational Einstein coefficients weighted by Py1$^-$ Boltzmann factors at $T = 300\,\text{K}$ allowing for population of $v = 1, 2, 3$ vibrational levels depending on the mode frequency, and with the outgoing electron kinetic energy corrected for the DBS binding energy. The resulting VAD spectrum, shown as the vertical sticks in Figure 3a, satisfactory accounts for the low-eKE vibrational structure. Because the rotational period of Py1$^-$ is at least several picoseconds, rotational autodetachment of the DBS is expected to be a minor decay channel.[3,35,42]

The valence-localized state to DBS internal conversion lifetime of $\tau_1 = 160 \pm 20\,\text{fs}$ is within the range of sub-picosecond values determined for cluster anions anions ($\approx 60\,\text{fs}$)[18] and a model biochromophore anion ($\approx 600\,\text{fs}$),[11] although the latter involved extensive nuclear motion to induce coupling. The τ_1 value is comparable with the autodetachment lifetime for the S$_1$ electronic state in 2-naphthoxide ($T \approx 300\,\text{K}$) at $130 \pm 10\,\text{fs}$,[43] a molecule which is structurally equivalent to Py1$^-$ minus two aromatic rings. Such an ultrafast internal

conversion is affected by strong coupling between the vibrational modes of the two electronic states. This coupling may be because of a conical intersection seam close to the Franck-Condon geometry,[44] or because of a high transition probability in the framework of Fermi's golden rule due to the overlap of DBS vibrations with the S_1 band. The DBS lifetime, $\tau_2 = 11 \pm 2\,\text{ps}$, is consistent with measured VAD lifetimes for $v = 1$ DBS vibrations (1.4 to 34 ps) in cryocooled phenoxide.[20] While the influence of the initial temperature of $Py1^-$ is certainly a direction for future work, all measurements to date on vibrationally excited DBSs have reported lifetimes in the 1–40 ps range.

This work has shown efficient internal conversion between a valence-localized excited state and a DBS. The observation here for a 'rigid' molecule is important in establishing the process as a general non-adiabatic decay mechanism. Specifically, such internal conversions to a DBS (or related correlation-bound state) have been previously observed in only "floppy" cluster anions,[18,45,46] and molecular anions with low-energy degrees of freedom.[11] While efficient coupling between valence and non-valence states (Rydberg states) in neutral molecules is well known,[47] little is known about the analogous processes in anions. Because strong coupling inherently facilitates bidirectional dynamics, efficient internal conversion from the DBS to valence-localized state may occur in instances when the valence state is slightly lower in energy than the DBS.[19]

Internal conversion between a valence-localized state and the DBS has implications for interstellar anion abundance and lifecycle. Briefly, while the existence of PAH-based molecules in space is largely based on circumstantial evidence,[48–51] the current consensus in the astronomical community is that >10% of galactic carbon is tied up as PAHs. The recent assignment of benzonitrile[52] and isomers of cyanonaphthalene[53] to interstellar rotational lines lends compelling evidence for the existence of hetero-PAHs in space. The accepted interstellar anion formation mechanism originally postulated by Sarre[7] involves the capture of a low energy electron into a DBS followed by internal conversion and liberation of internal energy through radiative emission, or through dissociation to generate a smaller anion.

Assuming this model, pristine PAH anions and dehydrogenated derivatives should not be present in space because they have a zero or an inadequate molecular dipole moment to support a DBS; a heteroatom (e.g. N or O) or polar functional group such as –CN (cyano) is necessary to achieve $|\mu| > 2.0\,\text{D}$.[54] Furthermore, even though the parent neutral molecule in space would exist at $T \approx$ 4–20 K, the internal energy of a nascent anion formed through the Sarre mechanism will be above the detachment threshold and therefore susceptible to VAD. For stable interstellar anion formation, internal conversion to the S_0 electronic state must occur more rapidly than VAD; however, no such internal conversion was observed for cryocooled phenoxide,[20] 2-naphthoxide at $T \approx 300\,\text{K}$,[43] or Py1^- at $T \approx 300\,\text{K}$ in this study. We propose that the lack of internal conversion to the S_0 state is due to the absence of valence-bound excited states situated below the DBS,[11,16,17,55] which can couple with the DBS through active vibrations.[56] As an example, the C_{2n}H^- ($n = 2 - 4$) series accounts for half of the anions currently known to exist in space,[8,57] each of which possess valence-bound excited states in the vicinity of the DBS.[58] For oxygenated PAHs like Py1, because the electron detachment energy and density of excited electronic states increases with the number of aromatic rings, a derivative with six to eight aromatic rings should achieve an electronic structure similar to the C_{2n}H^- ($n = 2-4$) series and potentially facilitate internal conversion to the S_0 electronic state. Following on from this hypothesis, we expect that hetero-PAH molecules that do not have valence-bound excited states are unlikely to be significant carriers of negative charge in space.

In summary, this work has provided the first direct evidence for a sub-picosecond internal conversion to the DBS in a 'rigid' anion and where time-resolved experiments allow excitation of a specific vibronic transition. In turn, the DBS decays over the picosecond timescale through vibrational autodetachment and with no evidence for internal conversion to the ground electronic state. Of particular note is the clear evolution of the photoelectron angular distribution during the internal conversion process to form a dipole-bound state. While these internal conversion dynamics are likely commonplace in anionic systems, including in

interstellar anion formation and coupling of solutes with solvated electrons, the ultrafast timescales and lack of distinct spectral signatures in single-photon spectroscopies restrict clear observations. The present strategy for characterizing the ultrafast internal conversion dynamics from the S_1 state to the DBS, or *vice versa* from the DBS, can be applied to any anion possessing excited states that are accessible with femtosecond lasers.

Supporting Information Available

Experimental methods; Photodepletion spectrum; Theoretical methods; Calculated vibrational frequencies; Franck-Condon-Herzberg-Teller simulations.

Acknowledgements

of East Anglia.

Conflicts of interest

There are no conflicts to declare.

Author contributions

The investigation was proposed and coordinated by JNB. Photodetachment spectroscopy experiments were performed by JNB in the laboratory of EJB. Time-resolved photoelectron spectroscopy experiments were performed by JNB, CSA, CJC and JAG in the laboratory of JRRV. Photodepletion experiments were performed by JNB and MHS. Electronic structure calculations were performed by JNB. The manuscript was prepared by JNB and discussed by all authors.

Data availability

The data that support the findings of this study are available from the corresponding author upon reasonable request.

References

(1) Fermi, E.; Teller, E. The Capture of Negative Mesotrons in Matter. *Phys. Rev.* **1947**, *72*, 399–408.

(2) Garrett, W. R. Critical Binding of an Electron to a Rotationally Excited Dipolar System. *Phys. Rev. A* **1971**, *3*, 961–972.

(3) Simons, J. Molecular Anions. *J. Phys. Chem. A* **2008**, *112*, 6401–6511.

(4) Qian, C.-H.; Zhu, G.-Z.; Wang, L.-S. Probing the Critical Dipole Moment To Support Excited Dipole-Bound States in Valence-Bound Anions. *J. Phys. Chem. Lett.* **2019**, *10*, 6472–6477.

(5) Jordan, K. D.; Wang, F. Theory of Dipole-Bound Anions. *Ann. Rev. Phys. Chem.* **2003**, *54*, 367–396.

(6) Hammer, N. I.; Diri, K.; Jordan, K. D.; Desfrancois, C.; Compton, R. N. Dipole-Bound Anions of Carbonyl, Nitrile, and Sulfoxide Containing Molecules. *J. Chem. Phys.* **2003**, *119*, 3650.

(7) Sarre, P. J. The Diffuse Interstellar Bands: A Dipole-Bound State Hypothesis. *Mon. Not. Royal Astron. Soc.* **2000**, *313*, L14–L16.

(8) Millar, T. J.; Walsh, C.; Field, T. A. Negative Ions in Space. *Chem. Rev.* **2017**, *117*, 1765–1795.

(9) Guthe, F.; Tulej, M.; Pachkov, M. V.; Maier, J. P. Photodetachment Spectrum of l-$C_3H_2^-$: The Role of Dipole Bound States for Electron Attachment in Interstellar Clouds. *Astrophys. J.* **2001**, *555*, 466–471.

(10) Sanche, L. Low Energy Electron-Driven Damage in Biomolecules. *Eur. Phys. J. D* **2005**, *35*, 367–390.

(11) Bull, J. N.; Anstöter, C. S.; Verlet, J. R. R. Ultrafast Valence to Non-Valence Excited State Dynamics in a Common Anionic Chromophore. *Nat. Comm.* **2019**, *10*, 5820.

(12) Anusiewicz, I.; Skurski, P.; Simons, J. Fate of Dipole-Bound Anion States when Hydrated. *J. Phys. Chem. A* **2020**, *124*, 2064–2076.

(13) Albeck, Y.; Lunny, K. G.; Benitez, Y.; Shin, A. J.; Strasser, D.; Continetti, R. E. Resonance-Mediated Below-Threshold Delayed Photoemission and Non-

Franck–Condon Photodissociation of Cold Oxyallyl Anions. *Angew. Chem. Int. Ed.* **2019**, *131*, 5366.

(14) Kang, D. H.; Kim, J.; Kim, S. K. Recapture of the Nonvalence Excess Electron into the Excited Valence Orbital Leads to the Chemical Bond Cleavage in the Anion. *J. Phys. Chem. Lett.* **2021**, *12*, 6383–6388.

(15) Liu, H.-T.; Ning, C.-G.; Huang, D.-L.; Dau, P. D.; Wang, L.-S. Observation of Mode-Specific Vibrational Autodetachment From Dipole-Bound States of Cold Anions. *Angew. Chem. Int. Ed.* **2013**, *52*, 8976–8979.

(16) King, S. B.; Yandell, M. A.; Neumark, D. M. Time-Resolved Photoelectron Imaging of the Iodide–Thymine and Iodide–Uracil Binary Cluster Systems. *Faraday Discuss.* **2013**, *163*, 59–72.

(17) Yandell, M. A.; King, S. B.; Neumark, D. M. Decay Dynamics of Nascent Acetonitrile and Nitromethane Dipole-Bound Anions Produced by Intracluster Charge-Transfer. *J. Chem. Phys.* **2014**, *140*, 184317.

(18) Bull, J. N.; West, C. W.; Verlet, J. R. R. Ultrafast Dynamics of Formation and Autodetachment of a Dipole-Bound State in an Open-Shell π-Stacked Dimer Anion. *Chem. Sci.* **2016**, *7*, 5352–5361.

(19) Kunin, A.; Neumark, D. M. Time-Resolved Radiation Chemistry: Femtosecond Photoelectron Spectroscopy of Electron Attachment and Photodissociation Dynamics in Iodide–Nucleobase Clusters. *Phys. Chem. Chem. Phys.* **2019**, *21*, 7239–7255.

(20) Kang, D. H.; An, S.; Kim, S. K. Real-Time Autodetachment Dynamics of Vibrational Feshbach Resonances in a Dipole-Bound State. *Phys. Rev. Lett.* **2020**, *125*, 093001.

(21) Qian, C.-H.; Zhang, Y.-R.; Yuan, D.-F.; Wang, L.-S. Photodetachment Spectroscopy

and Resonant Photoelectron Imaging of Cryogenically Cooled 1-pyrenolate. *J. Chem. Phys.* **2021**, *154*, 094308.

(22) Jiang, W.; Li, Y.; Wang, Z. Heteroarenes as High Performance Organic Semiconductors. *Chem. Soc. Rev.* **2013**, *42*, 6113–6127.

(23) Bouwman, J.; Paardekooper, D. M.; Cuppen, H. M.; Linnartz, H.; Allamandola, L. J. Real-Time Optical Spectroscopy of Vacuum Ultraviolet Irradiated Pyrene:H_2O Interstellar Ice. *Astrophys. J.* **2009**, *700*, 56–62.

(24) Bouwman, J.; Cuppen, H. M.; Bakker, A.; Allamandola, L. J.; Linnartz, H. Photochemistry of the PAH Pyrene in Water Ice: The Case for Ion-Mediated Solid-State Astrochemistry. *Astron. Astrophys.* **2010**, *511*, A33.

(25) Bernstein, M. P.; Sandford, S. A.; Allamandola, L. J.; Gillette, J. S.; Clemett, S. J.; Zare, R. N. UV Irradiation of Polycyclic Aromatic Hydrocarbons in Ices: Production of Alcohols, Quinones, and Ethers. *Science* **1999**, *283*, 1135–1138.

(26) Bernstein, M. P.; Moore, M. H.; Elsila, J. E.; Sandford, S. A.; Allamandola, L. J.; Zare, R. N. Side Group Addition to the Polycyclic Aromatic Hydrocarbon Coronene by Proton Irradiation in Cosmic Ice Analogs. *Astrophys. J. Lett.* **2002**, *582*, L25–L29.

(27) Bernstein, M. P.; Elsila, J. E.; Dworkin, J. P.; Sandford, S. A.; Allamandola, L. J.; Zare, R. N. Side Group Addition to the Polycyclic Aromatic Hydrocarbon Coronene by Ultraviolet Photolysis in Cosmic Ice Analogs. *Astrophys. J.* **2002**, *576*, 1115–1120.

(28) Gudipati, M. S.; Yang, R. In Situ Probing of Radiation-Induced Processing of Organics in Astrophysical Ice Analogs – Novel Laser Desorption Laser Ionization Time-of-Flight Mass Spectrometric Studies. *Astrophys. J.* **2012**, *756*, L24.

(29) Cook, A. M.; Ricca, A.; Mattioda, A. L.; Bouwman, J.; Roser, J.; Linnartz, H.; Bregman, J.; Allamandola, L. J. Photochemistry of Polycyclic Aromatic Hydrocarbons in

Cosmic Water Ice: The Role of PAH Ionization and Concentration. *Astrophys. J.* **2015**, *799*, 14.

(30) Taylor, H. S.; Nazaroff, G. V.; Golebiewski, A. Qualitative Aspects of Resonances in Electron-Atom and Electron-Molecule Scattering, Excitation, and Reactions. *J. Chem. Phys.* **1966**, *45*, 2872–2888.

(31) Eppink, A. T. J. B.; Parker, D. H. Velocity Map Imaging of Ions and Electrons Using Electrostatic Lenses: Application in Photoelectron and Photofragment Ion Imaging of Molecular Oxygen. *Rev. Sci. Instrum.* **1997**, *68*, 3477–3484.

(32) Roberts, G. M.; Nixon, J. L.; Lecointre, J.; Wrede, E.; Verlet, J. R. R. Toward Real-Time Charged-Particle Image Reconstruction Using Polar Onion-Peeling. *Rev. Sci. Instrum.* **2009**, *80*, 053104.

(33) Zare, R. N. Photoejection Dynamics. *Mol. Photochem.* **1972**, *4*, 1–37.

(34) West, C. W.; Bull, J. N.; Antonkov, E.; Verlet, J. R. R. Anion Resonances of para-Benzoquinone Probed by Frequency-Resolved Photoelectron Imaging. *J. Phys. Chem. A* **2014**, *118*, 11346–11354.

(35) Simons, J. Ejecting Electrons from Molecular Anions via Shine, Shake/Rattle, and Roll. *J. Phys. Chem. A* **2020**, *124*, 8778–8797.

(36) Hanggi, D.; Carr, P. W. Errors in Exponentially Modified Gaussian Equations in the Literature. *Anal. Chem.* **1985**, *57*, 2394–2395.

(37) Simons, J. Propensity Rules For Vibration-Induced Electron Detachment of Anions. *J. Am. Chem. Soc.* **1981**, *103*, 3971–3976.

(38) Acharya, P. K.; Kendall, R. A.; Simons, J. Vibration-Induced Electron Detachment in Molecular Anions. *J. Am. Chem. Soc.* **1984**, *106*, 3402–3407.

(39) Zhu, G.-Z.; Qian, C.-H.; Wang, L.-S. Dipole-Bound Excited States and Resonant Photoelectron Imaging of Phenoxide and Thiophenoxide Anions. *J. Chem. Phys.* **2018**, *149*, 164301.

(40) Zhu, G.-Z.; Wang, L.-S. High-Resolution Photoelectron Imaging and Resonant Photoelectron Spectroscopy via Noncovalently Bound Excited States of Cryogenically Cooled Anions. *Chem. Sci.* **2019**, *10*, 9409–9423.

(41) Anstöter, C. S.; Mensa-Bonsu, G.; Nag, P.; Ranković, M.; P., R. K. T.; Boichenko, A. N.; Bochenkova, A. V.; Fedor, J.; Verlet, J. R. Mode-Specific Vibrational Autodetachment Following Excitation of Electronic Resonances by Electrons and Photons. *Phys. Rev. Lett.* **2020**, *124*, 203401.

(42) Walthall, D. A.; Karty, J. M.; Brauman, J. I. Molecular Rotations and Dipole-Bound State Lifetimes. *J. Phys. Chem. A* **2005**, *109*, 8794–8799.

(43) Ashworth, E. K.; Anstöter, C. S.; Verlet, J. R. R.; Bull, J. N. Autodetachment Dynamics of 2-naphthoxide and Implications for Astrophysical Anion Abundance. *Phys. Chem. Chem. Phys.* **2021**, *23*, 5817–5823.

(44) Worth, G. A.; Cederbaum, L. S. Beyond Born-Oppenheimer: Molecular Dynamics Through a Conical Intersection. *Ann. Rev. Phys. Chem.* **2004**, *55*, 127–158.

(45) Bull, J. N.; Verlet, J. R. R. Observation and Ultrafast Dynamics of a Nonvalence Correlation-Bound State of an Anion. *Sci. Adv.* **2017**, *3*, e1603106.

(46) Rogers, J. P.; Anstöter, C. S.; Verlet, J. R. R. Ultrafast Dynamics of Low-Energy Electron Attachment via a Non-Valence Correlation-Bound State. *Nat. Chem.* **2018**, *10*, 341–346.

(47) Gallagher, T. F. *Rydberg Atoms*; Cambridge University Press, 1994.

(48) Ruiterkamp, R.; Halasinski, T.; Salama, F.; Foing, B. H.; Allamandola, L. J.; Schmidt, W.; Ehrenfreund, P. Spectroscopy of Large PAHs. *Astron. Astrophys.* **2002**, *390*, 1153–1170.

(49) Lagache, G.; Dole, H.; Puget, J.-L.; Perez-Gonzalez, P. G.; Floc'h, E. L.; Rieke, G. H.; Papovich, C.; Egami, E.; Alonso-Herrero, A.; Engelbracht, C. W. et al. Polycyclic Aromatic Hydrocarbon Contribution to the Infrared Output Energy of the Universe at z $\simeq$ 2. *Astrophys. J. Supp. Ser.* **2004**, *154*, 112–117.

(50) Mulas, G.; Malloci, G.; Joblin, C.; Toublanc, D. Estimated IR and Phosphorescence Emission Fluxes for Specific Polycyclic Aromatic Hydrocarbons in the Red Rectangle. *Astron. Astrophys.* **2006**, *446*, 537–549.

(51) Bauschlicher, C. W.; Ricca, A.; Boersma, C.; Allamandola, L. J. The NASA Ames PAH IR Spectroscopic Database: Computational Version 3.00 with Updated Content and the Introduction of Multiple Scaling Factors. *Astrophys. J. Supp. Ser.* **2018**, *234*, 32.

(52) McGuire, B. A.; Burkhardt, A. M.; Kalenskii, S.; Shingledecker, C. N.; Remijan, A. J.; Herbst, E.; McCarthy, M. C. Detection of the Aromatic Molecule Benzonitrile (c-C_6H_5CN) in the Interstellar Medium. *Science* **2018**, *359*, 202–205.

(53) McGuire, B. A.; Loomis, R. A.; Burkhardt, A. M.; Lee, K. L. K.; Shingledecker, C. N.; Charnley, S. B.; Cooke, I. R.; Cordiner, M. A.; Herbst, E.; Kalenskii, S. et al. Detection of Two Interstellar Polycyclic Aromatic Hydrocarbons via Spectral Matched Filtering. *Science* **2021**, *371*, 1265–1269.

(54) Theis, M. L.; Candian, A.; Tielens, A. G. G. M.; Lee, T. J.; Fortenberry, R. C. Electronically Excited States of PANH Anions. *Phys. Chem. Chem. Phys.* **2015**, *17*, 14761–14772.

(55) Bull, J. N.; West, C. W.; Verlet, J. R. R. On the Formation of Anions: Frequency-, Angle-, and Time-Resolved Photoelectron Imaging of the Menadione Radical Anion. *Chem. Sci.* **2015**, *6*, 1578–1589.

(56) Gutsev, G. L.; Bartlett, R. J. A Theoretical Study of the Valence- and Dipole-Bound States of the Nitromethane Anion. *J. Chem. Phys.* **1996**, *105*, 8785–8792.

(57) McCarthy, M. C.; Gottlieb, C. A.; Gupta, H.; Thaddeus, P. Laboratory and Astronomical Identification of the Negative Molecular Ion C_6H^-. *Astrophys. J.* **2006**, *652*, L141–L144.

(58) Pino, T.; Tulej, M.; Güthe, F.; Pachkov, M.; Maier, J. P. Photodetachment Spectroscopy of the $C_{2n}H^-$ (n=2–4) Anions in the Vicinity of Their Electron Detachment Threshold. *J. Chem. Phys.* **2002**, *116*, 6126–6131.